

POLYSEMOUS LANGUAGE GAUSSIAN SPLATTING VIA MATCHING-BASED MASK LIFTING

Jiayu Ding¹, Xinpeng Liu¹, Zhiyi Pan², Shiqiang Long³, Ge Li^{1†}

¹School of Electronic and Computer Engineering, Peking University

²School of Computer Science and Technology, Tianjin University

³Guangdong Bohua UHD Innovation Center Co., Ltd.

{jyding25@stu, lxpeng@stu, GeLi@}.pku.edu.cn

zhypan@tju.edu.cn, longsq@bohuauid.com

ABSTRACT

Lifting 2D open-vocabulary understanding into 3D Gaussian Splatting (3DGS) scenes is a critical challenge. However, mainstream methods suffer from three key flaws: (i) their reliance on costly per-scene retraining prevents plug-and-play application; (ii) their restrictive monosemous design fails to represent complex, multi-concept semantics; and (iii) their vulnerability to cross-view semantic inconsistencies corrupts the final semantic representation. To overcome these limitations, we introduce MUSplat, a training-free framework that abandons feature optimization entirely. Leveraging a pre-trained 2D segmentation model, our pipeline generates and lifts multi-granularity 2D masks into 3D, where we estimate a foreground probability for each Gaussian point to form initial object groups. We then optimize the ambiguous boundaries of these initial groups using semantic entropy and geometric opacity. Subsequently, by interpreting the object’s appearance across its most representative viewpoints, a Vision-Language Model (VLM) distills robust textual features that reconciles visual inconsistencies, enabling open-vocabulary querying via semantic matching. By eliminating the costly per-scene training process, MUSplat reduces scene adaptation time from hours to mere minutes. On benchmark tasks for open-vocabulary 3D object selection and semantic segmentation, MUSplat outperforms established training-based frameworks while simultaneously addressing their monosemous limitations.

1 INTRODUCTION

Open-vocabulary 3D scene understanding enables the parsing of 3D scenes with arbitrary natural language queries, moving beyond the limitations of predefined categories to offer enhanced generalization and richer semantics for applications like autonomous driving and robotics. The primary challenge in this domain lies in finding an efficient and effective 3D scene representation. Traditional methods such as voxels, point clouds, and meshes, while useful for structure modeling, struggle with the trade-off between detail and computational expense. Recently, 3D Gaussian Splatting (3DGS) (Kerbl et al., 2023) has provided a compelling solution by merging the explicit structure of traditional methods with the efficiency of neural techniques. It achieves high-quality modeling and rendering while maintaining high rendering speeds, making it an ideal foundation for next-generation 3D scene understanding.

More recently, several methods have leveraged 3DGS for point-level open-vocabulary 3D scene understanding, achieving remarkable results. Current research is largely dominated by the **training**-based contrastive learning paradigm (Li et al., 2025; Wu et al., 2024), as illustrated in Fig. 1(a). These methods rely on a laborious optimization pipeline: they first perform tens of thousands of mask-guided contrastive learning iterations to embed semantic features into each Gaussian, followed by clustering and post-processing steps to achieve feature-language alignment. Furthermore, a minority of studies (Jun-Seong et al., 2025) have explored a feature projection paradigm, which

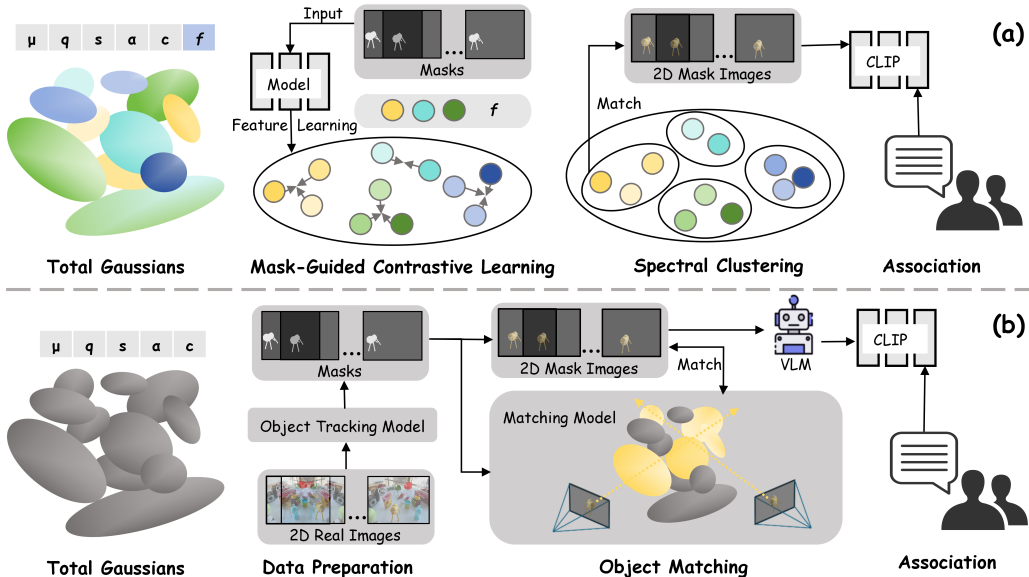


Figure 1: Pipelines for open-vocabulary understanding of 3D Gaussian scenes. (a) Training-based approaches: semantic features are learned via mask-guided contrastive learning, followed by clustering and post-processing. (b) Our training-free matching-based approach: semantic associations are determined directly through matching, without feature learning.

trains a specialized model to compress Contrastive Language-Image Pre-training (CLIP) (Radford et al., 2021) features and subsequently assigns these compressed features to the 3D Gaussians for open-vocabulary understanding. While these approaches have shown promising results, we argue that they suffer from three critical limitations that hinder their performance and practical deployment: **1) Reliance on Expensive Optimization:** The dominant contrastive learning paradigm requires tens of thousands of iterations for per-scene semantic optimization. Similarly, the feature projection paradigm necessitates pre-training a specialized feature compression model. Both pathways introduce significant time and computational overhead, undermining the efficiency advantages of 3DGS. **2) Deficient Semantic Representation:** Existing methods lack richness and precision in their semantic representations. On one hand, the prevailing contrastive methods are restricted by a “one-to-one” semantic assignment, attributing a single semantic concept to each Gaussian. This makes them incapable of capturing polysemy, the phenomenon where a single point may belong to multiple semantic concepts (e.g., a desk point being simultaneously “desk”, “wooden”, and “furniture”). On the other hand, feature projection methods suffer from degraded feature quality. Their reliance on lossy feature compression often impairs the model’s fine-grained understanding and semantic discriminability. **3) Fragile Multi-view Feature Aggregation:** A critical yet often overlooked issue is the viewpoint variance of CLIP’s image features, where the same object instance yields significantly inconsistent embeddings across different viewpoints. Current aggregation strategies fail to robustly handle view-dependent variations. For instance, mainstream methods typically assign single-view masked CLIP features to Gaussians, while projection-based approaches perform a weighted average of multi-view features; both tactics lead to inaccurate 3D semantic representations. These concerns motivate the central question of our work: “Can we construct a framework for open-vocabulary understanding of 3D Gaussian scenes that robustly aggregates multi-view features, supports polysemous representations, and operates without requiring any additional training?”

To answer this question, we introduce **Matching-based Understanding with 3D Gaussian Splatting (MUSplat)**, a novel training-free framework that bypasses feature optimization entirely. As illustrated in Fig. 1(b), our framework determines the semantics of each Gaussian through a **matching** mechanism, which is inherently designed to handle polysemy and operate without per-scene retraining. Our framework first lifts 2D masks to form 3D object groups, then refines their boundaries with neutral point processing for enhanced precision. After that, We leverage a Vision-Language Model (VLM) to generate textual features for each object, enabling precise language-based retrieval. Our contributions are summarized as follows:

- We introduce MUSplat, a training-free and polysemy-aware framework for open-vocabulary understanding in 3D Gaussian scenes.
- We propose an Object-level Grouping method that achieves precise 3D instance grouping by probabilistically lifting 2D masks and subsequently refining ambiguous boundaries with a neutral point processing mechanism.
- We present a VLM-based distillation technique that forges a robust and unified textual representation from inconsistent multi-view visual features.

2 RELATED WORKS

2.1 PRELIMINARY: 3D GAUSSIAN SPLATTING

3D Gaussian Splatting (3DGS) (Kerbl et al., 2023) models 3D scenes with explicit 3D Gaussians, enabling high-quality, real-time rendering. It represents a scene as a collection of 3D Gaussians $\mathcal{G} = \{g_i\}_{i=1}^N$, each defined by its position, covariance (governing scale and orientation), color, and opacity. To generate a 2D image, these 3D Gaussians are projected onto an image plane and then blended in a depth-sorted order via “splatting”. The final color $C(p)$ for any pixel p is determined through alpha compositing (Munkberg et al., 2022):

$$C(p) = \sum_{i=1}^{|\mathcal{G}_p|} c_{g_i^p} \alpha_{g_i^p} \prod_{j=1}^{i-1} (1 - \alpha_{g_j^p}), \quad (1)$$

where $c_{g_i^p}$ and $\alpha_{g_i^p}$ are the color and opacity of the i -th Gaussian in the sorted set for pixel p . The product term, $\prod_{j=1}^{i-1} (1 - \alpha_{g_j^p})$, calculates the accumulated transmittance, which represents the light that reaches the i -th Gaussian after passing through all prior ones.

2.2 OPEN VOCABULARY UNDERSTANDING BASED ON 3DGS

Prevailing methods for semanticizing 3DGS for open-vocabulary understanding follow two primary paradigms: pixel-based and point-based. Pixel-based methods employ a “render-then-match” paradigm: they first render the entire scene into dense 2D feature maps and subsequently perform semantic matching in the image space. In contrast, point-based methods adopt a “match-then-render” strategy, first identifying a sparse set of semantically relevant 3D points and then rendering only this pre-filtered subset.

In pixel-based methods, Feature-3DGS (Zhou et al., 2024) distills semantic features from 2D foundation models into 3DGS, enabling fast semantic rendering. LEGaussians (Shi et al., 2024) adds uncertainty and semantic to each Gaussian and compares rendered semantic maps with quantized CLIP and DINO features. LangSplat (Qin et al., 2024) learns language features in a scene-specific latent space and renders them as semantic maps. GS-Grouping (Ye et al., 2024) assigns a compact identity encoding to each Gaussian and leverages masks from the Segment Anything Model (SAM) (Kirillov et al., 2023) for supervision. GOI (Qu et al., 2024) introduces an optimizable semantic hyperplane to separate pixels relevant to language queries, improving open-vocabulary accuracy.

However, these methods rely on rendered 2D semantic maps, so reasoning remains in 2D. They lack awareness of 3D structure and are thus less suited for tasks requiring direct 3D interaction, such as embodied intelligence. To overcome these limitations, point-based methods have been proposed. These approaches operate on a foundational “select-then-render” pipeline. OpenGaussian (Wu et al., 2024) uses SAM masks to learn instance features with 3D consistency, introduces a two-stage codebook for feature discretization, and links 3D points with 2D masks and CLIP features for open-vocabulary selection. InstanceGaussian (Li et al., 2025), based on Scaffold-GS (Lu et al., 2024), jointly learns appearance and semantics and adaptively aggregates instances, reducing semantic–appearance misalignment. Dr.Splat (Jun-Seong et al., 2025) trains a feature compressor for each scene and assigns compressed CLIP features to every Gaussian. All these approaches rely on computationally expensive iterative training. Our model instead follows a training-free matching framework that establishes a semantic link between 3D Gaussian points and a query by directly matching their uncompressed CLIP features.

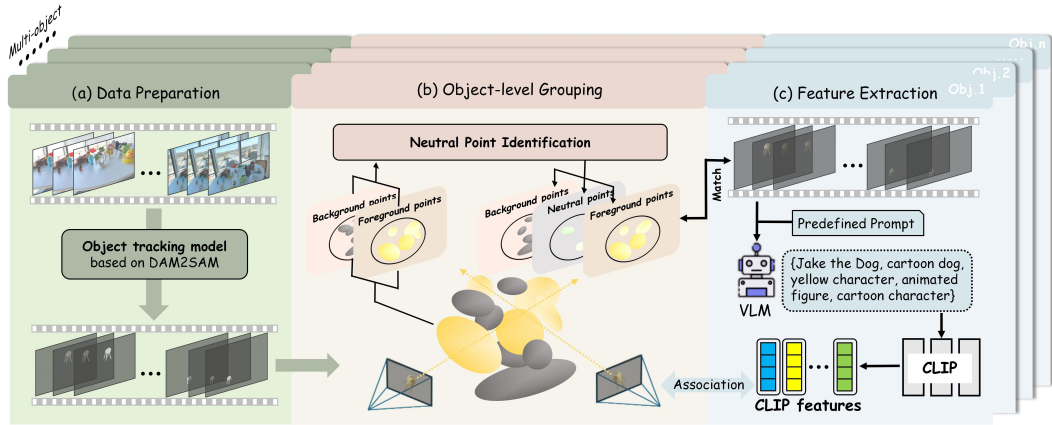


Figure 2: Overview of our method. (a) Multi-view 2D segmentation masks are first extracted from the input scene. (b) Based on these masks, our method lifts the objects into 3D point groups via back-projection, refining their boundaries by filtering ambiguous neutral points. (c) Each refined group is then grounded by using a VLM to generate textual hypotheses from its key views, which are encoded into semantic features via a CLIP text encoder.

3 METHOD

We propose a training-free pipeline for point-level 3D open-vocabulary semantic segmentation, as shown in Fig. 2. Our method takes a pre-trained 3DGS scene representation and its corresponding image sequence as input. First, the Data Preparation stage (§3.1) generates multi-view, multi-granularity object masks. Next, the Object-level Grouping stage (§3.2) links 2D masks to 3D Gaussian points and purifies the resulting object boundaries by identifying and excluding ambiguous neutral points. Finally, the Instance Feature Extraction stage (§3.3) uses a VLM to extract textual features for each object, enabling alignment with open-vocabulary queries.

3.1 DATA PREPARATION

Our goal is to extract a comprehensive set of multi-view segmentation masks for all objects in a scene. To this end, we first employ SAM on the initial frame, I_0 , leveraging its ability to produce object masks at three distinct granularity levels (e.g., part, object, scene). To ensure stable tracking throughout the sequence, especially in complex scenes with visually similar distractors, we employ the DAM2SAM (Videnovic et al., 2025) model. Its specialized distractor-aware memory is crucial for maintaining accurate object identities where other trackers might fail. To capture new objects that appear later, we introduce a periodic detection mechanism that re-segments the scene at fixed intervals and identifies new instances based on a minimal IoU overlap criterion with existing tracks. The entire pipeline, from tracking to new object detection, is executed independently for each of the three granularity levels to yield a complete and hierarchical set of masks.

Our pipeline is designed for robustness, as potential data preparation artifacts, such as tracking failures or re-identification errors, are gracefully handled by our downstream object grouping and query matching modules. This design minimizes the requirements for perfect input data.

3.2 OBJECT-LEVEL GROUPING

To precisely group 3D Gaussian instances, we resolve ambiguous boundary points that corrupt segmentation using a two-stage, coarse-to-fine strategy. We first identify the object’s high-confidence core via mask back-projection, then refine its boundaries by identifying and excluding ambiguous points with our neutral point processing module, ensuring a clean result.

Initial 3D Grouping via Mask Back-projection. We link 2D masks to 3D Gaussian points by back-projecting them to estimate a per-point foreground probability. For each object, we process its multi-view masks, first discarding any null (entirely black) masks from viewpoints where the object is unseen. For each valid mask, we then cast a ray through each pixel r and sum the contributions of

all intersected Gaussians. The contribution of the j -th Gaussian G_j along ray r is determined by its accumulated transmittance and opacity, defined as:

$$w(r, G_j) = T(r, G_j) \cdot \alpha(r, G_j), \quad (2)$$

where $T(r, G_j)$ denotes the accumulated transmittance up to G_j , and $\alpha(r, G_j)$ is its effective opacity. To ensure design consistency, we define the weight $w(r, G_j)$, representing the contribution of Gaussian G_j to pixel r , to be identical to the forward color rendering weight of 3DGS given in Eq. 1.

For each 3D Gaussian point G_j , we compute its total foreground (W_1) and background (W_0) weights by aggregating contributions from multi-view 2D masks:

$$W_k(G_j) = \sum_{v \in \mathcal{V}} \sum_{r \in \mathcal{P}_v} \delta(m_v(r) - k) \cdot w_v(r, G_j), \quad k \in \{0, 1\}, \quad (3)$$

where \mathcal{V} is the set of visible views, \mathcal{P}_v the pixels in a view, $m_v(r)$ the mask value, $\delta(\cdot)$ the indicator function, and $w_v(r, G_j)$ the contribution weight. Based on these weights, we form an initial set of foreground points, \mathcal{F} , using a simple hard assignment: $\mathcal{F} = \{G_j \mid W_1(G_j) > W_0(G_j)\}$. All remaining points are consequently assigned to the background.

Neutral Point Processing. During rendering, it is inevitable that some points lie at the boundaries between objects but do not semantically belong to any specific category. We refer to these points as neutral points. Their semantic assignment directly affects the accuracy of rendered object boundaries. Existing methods typically assume that each 3D Gaussian point belongs either to the foreground or to the background, i.e., every point has a clear semantic label. In practice, however, many points at boundaries are transitional and may not carry a well-defined semantic meaning. Such points should be considered neither foreground nor background. Our goal is to identify and exclude these neutral points from semantic supervision, thereby mitigating potential artifacts and improving the accuracy of the final segmentation.

To identify neutral points, we leverage multi-view semantic consistency. While points deep within an object are consistently labeled across views, those near boundaries often exhibit conflicting semantics. To quantify this ambiguity, we treat each viewpoint as providing a discrete semantic label for a given Gaussian point. Specifically, for each point p , we project its center into every visible view and record whether it lands inside (foreground) or outside (background) the corresponding 2D mask. This process yields a set of binary labels $\{l_v\}_{v \in \mathcal{V}}$ for each 3D point. The semantic entropy $H(p)$, which quantifies the disagreement among these discrete labels, is calculated as:

$$H(p) = - \left(\frac{V_f}{V} \log_2 \frac{V_f}{V} + \frac{V_b}{V} \log_2 \frac{V_b}{V} \right), \quad (4)$$

where V_f and V_b are the respective counts of foreground and background labels within the set $\{l_v\}_{v \in \mathcal{V}}$, and $V = |\mathcal{V}| = V_f + V_b$. Points with entropy $H(p)$ exceeding a threshold τ_h form an initial candidate set \mathcal{C} of ambiguous points.

This set \mathcal{C} is impure, containing both true neutral points used for smooth blending and mislabeled solid points that belong to an object’s surface. To distinguish them, we use a geometric property: opacity (α). Points on solid surfaces typically have high opacity, while transitional points used for anti-aliasing have low opacity. We filter \mathcal{C} based on this idea: if a point $p \in \mathcal{C}$ has an opacity $\alpha(p) > \tau_\alpha$, we classify it as a mislabeled solid point. These points, identified as part of a solid surface, are removed from the neutral candidate set \mathcal{C} , thereby retaining their initial classification as either foreground or background.

The remaining points in \mathcal{C} are confirmed as the final neutral point set, which is excluded from all semantic supervision. The final set of foreground points is thus defined by the expression $\mathcal{F} \setminus \mathcal{C}$. Likewise, the background set is refined by removing these same points. We use fixed values for the thresholds τ_h and τ_α across all experiments for simplicity and robustness.

3.3 INSTANCE FEATURE EXTRACTION

To enable open-vocabulary understanding, we extract semantic features for each 3D Gaussian cluster. As illustrated in Fig. 3(a), prevailing methods approach this by extracting visual features from multi-view masks of all objects. The semantic feature for a given 3D cluster is then derived by either selecting the feature from the most similar mask or by computing a weighted average of features

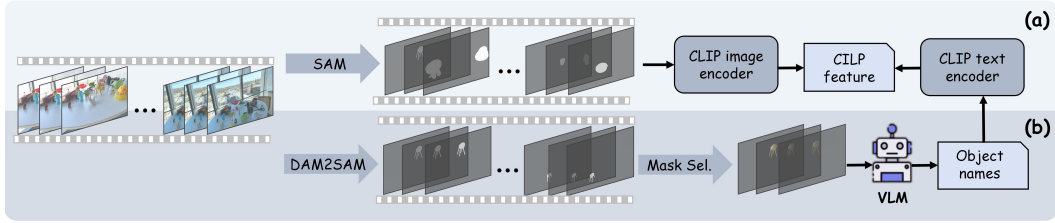


Figure 3: Comparison of 2D-3D Feature Association Pipelines. (a) Mainstream Method (via direct extraction): All object masks, typically generated by SAM, are used to directly extract CLIP image features. (b) Our Method (via semantic distillation): We leverage DAM2SAM to track a single instance. The top- N most visible masks are then interpreted by a VLM, distilling volatile visual appearances into a stable CLIP text representation derived from the generated object identity.

from all associated masks. However, this approach suffers from two major drawbacks. First, it overlooks the inherent semantic inconsistency across viewpoints. The visual features of the same object instance can vary significantly from different views, leading to a biased and inaccurate 3D semantic representation. Second, extracting and storing CLIP features for every object mask across all views incurs substantial computational and storage overhead, rendering the process inefficient. To avoid this, we propose semantic distillation: we use a VLM to interpret key views and generate textual hypotheses of the object’s identity. As shown in Fig. 3(b), this converts volatile visual appearances into a stable, canonical text representation, providing a robust foundation for open-vocabulary matching.

Specifically, for each object, we select the top- N masked views with the largest visible areas and feed them into a VLM along with a predefined text prompt, which instructs the model to generate a set of candidate names describing the object. Our framework is VLM-agnostic; for this study, we employ Gemini 2.5 Pro (Comanici et al., 2025), but other models can be readily substituted. Using a pre-trained CLIP text encoder, we encode the candidate names into a feature set \mathbf{Q} and an open-vocabulary text query into a feature vector \mathbf{s} . We quantify their semantic relevance using cosine similarity:

$$\text{sim}(\mathbf{s}, \mathbf{q}) = \frac{\mathbf{s} \cdot \mathbf{q}}{\|\mathbf{s}\| \|\mathbf{q}\|}, \quad (5)$$

We then form a set of matching features, \mathbf{Q}_m , by selecting all candidates whose similarity to the query exceeds a threshold η : $\mathbf{Q}_m = \{\mathbf{q} \in \mathbf{Q} \mid \text{sim}(\mathbf{s}, \mathbf{q}) > \eta\}$. The final segmentation for the query is the union of all 3D Gaussian point sets associated with the features in \mathbf{Q}_m .

4 EXPERIMENTS

4.1 OPEN-VOCABULARY OBJECT SELECTION IN 3D SPACE

Settings 1) Task. Given a text query as input, the task is to produce multi-view renderings of the semantically corresponding 3D instance(s). First, the textual feature of the input query is extracted using the CLIP model. Then, cosine similarity is computed between the query feature and the textual features of each instance, and the most similar instance(s) are selected. Finally, all 3D Gaussian points belonging to the selected instances are rendered into multi-view images through the 3DGS rasterization pipeline. **2) Baselines.** We compare our method with several recent representative approaches, including Dr.Splat (Jun-Seong et al., 2025), OpenGaussian (Wu et al., 2024), LangSplat (Qin et al., 2024), LEGaussian (Shi et al., 2024), InstanceGaussian (Li et al., 2025), Feature-3DGS (Zhou et al., 2024), GS-Grouping (Ye et al., 2024), and GOI (Qu et al., 2024). These approaches fall into the two primary categories of point-based and pixel-based methods. To provide a clear comparison, we detail the comparative aspects such as training time and search thresholds for these methods in Tab. 1. **3) Dataset.** We adopt the LERF (Kerr et al., 2023) dataset, annotated by LangSplat. This dataset consists of multi-view images capturing 3D scenes with long-tail objects and provides ground-truth 2D annotations for texture-level queries. For a fair comparison, we use the same predefined query texts as those used in OpenGaussian.

Results 1) Quantitative Evaluation. As shown in Tab. 2, our method achieves a new state-of-the-art (SOTA) result, outperforming the previous best-performing method by 10.7 mIoU. Although our

Table 1: This caption compares computational resources for the LERF *figurines* scene, including per-scene optimization time, peak VRAM use during object-level grouping, and storage for instance feature extraction. Our method is highly efficient, cutting CLIP feature storage from gigabytes to megabytes and using the least amount of VRAM. Notably, it is the only method that works directly in 3D without any training. Note that “–” marks methods that do not use CLIP features.

Method	Venue	Domain	Scene Opt.	Train Time	CLIP Feat. Stor.	Peak VRAM
LEGaussians	CVPR’24	2D	Required	~2h	~3GB	~20 GB
LangSplat	CVPR’24	2D	Required	~2h	~3GB	~20 GB
Feature-3DGS	CVPR’24	2D	Required	~1h	~3GB	~26 GB
GS-Grouping	ECCV’24	2D	Required	~1h	–	~28 GB
GOI	MM’24	2D	Required	~1h	–	~24 GB
OpenGaussian	NIPS’25	3D	Required	~1h	~3GB	~22 GB
InstanceGaussian	CVPR’25	3D	Required	~2h	~3GB	~24 GB
Dr.Splat	CVPR’25	3D	None	~1h	~3GB	~24 GB
Ours	–	3D	None	None	~3MB	~8 GB

Table 2: mIoU results for open-vocabulary object selection in 3D space on the LERF dataset. **Bold/Underline** indicates the best/second-best performance per category.

Method	Venue	ramen	teatime	figurines	Waldo_kitchen	Mean
Pixel-based						
LEGaussians	CVPR’24	46.0	60.3	40.8	39.4	46.6
LangSplat	CVPR’24	<u>51.2</u>	65.1	44.7	44.5	51.4
Feature-3DGS	CVPR’24	43.7	58.8	40.5	39.6	45.7
GS-Grouping	ECCV’24	45.5	60.9	40.0	38.7	46.3
GOI	MM’24	52.6	<u>63.7</u>	<u>44.5</u>	<u>41.4</u>	<u>50.6</u>
Point-based						
LangSplat-m	CVPR’24	6.1	16.6	8.3	8.3	9.8
LEGaussians-m	CVPR’24	15.8	19.3	18.0	11.8	16.2
OpenGaussian	NIPS’25	<u>31.0</u>	60.4	39.3	22.7	38.4
InstanceGaussian	CVPR’25	24.6	<u>63.4</u>	45.5	29.2	40.7
Dr.Splat(Top-40)	CVPR’25	24.7	57.2	<u>53.4</u>	39.1	43.6
Ours	–	45.6	64.4	66.4	40.9	54.3

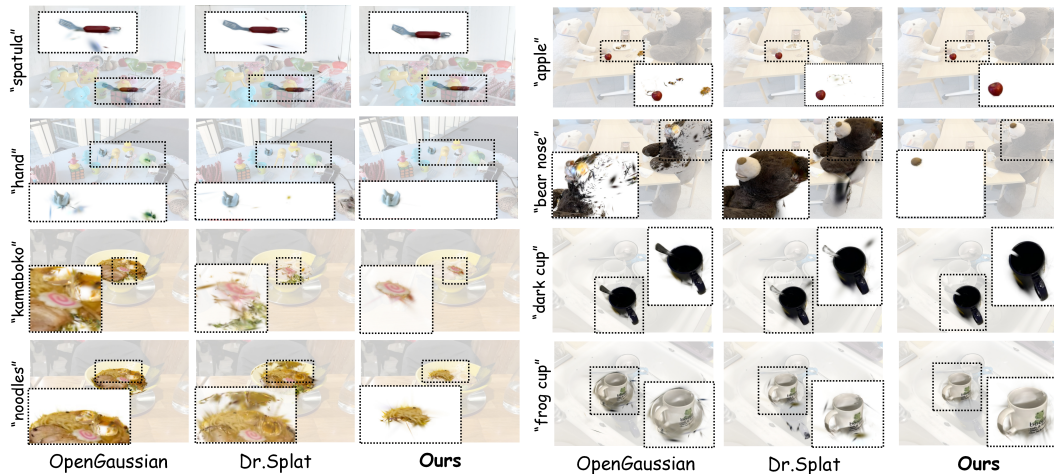


Figure 4: Qualitative results on object selection from the LERF dataset. OpenGaussian fails to separate nearby objects or maintain sharp boundaries, while InstanceGaussian struggles to capture fine-grained details. In contrast, our method correctly interprets fine-grained instructions to generate precise selections with well-defined boundaries.

Table 3: Quantitative results for open-vocabulary 3D semantic segmentation on the ScanNet dataset.

Method	Venue	19 classes		15 classes		10 classes	
		mIoU \uparrow	mAcc \uparrow	mIoU \uparrow	mAcc \uparrow	mIoU \uparrow	mAcc \uparrow
LangSplat-m	CVPR'24	3.8	9.1	5.4	13.2	8.4	22.1
LEGaussians-m	CVPR'24	1.6	7.9	4.6	16.1	7.7	24.9
OpenGaussian	NIPS'25	24.7	41.5	30.1	48.3	38.3	55.2
InstanceGaussian	CVPR'25	<u>40.7</u>	<u>54.0</u>	<u>42.5</u>	59.1	47.9	64.0
Dr.Splat(Top-40)	CVPR'25	29.6	47.7	38.2	<u>60.4</u>	<u>50.8</u>	<u>73.5</u>
Ours	–	45.5	58.4	47.2	61.7	53.7	74.9

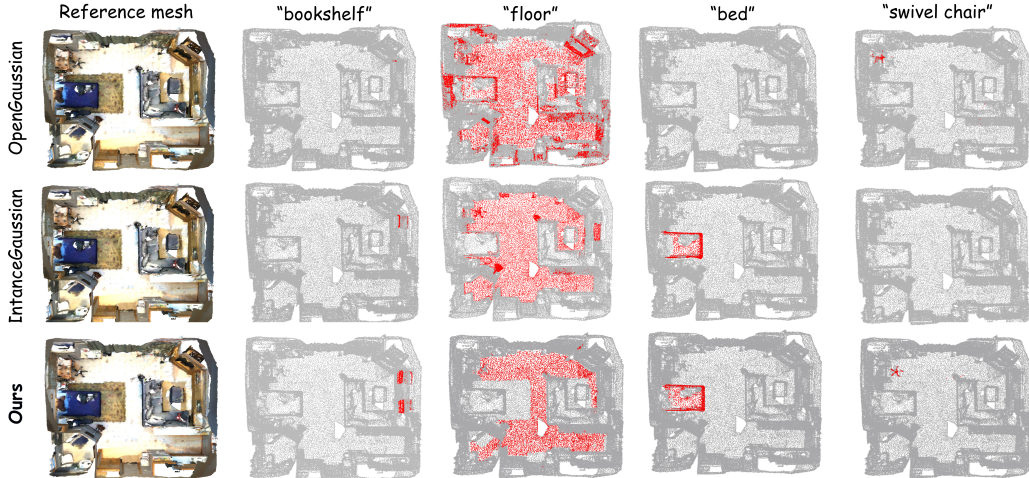


Figure 5: Qualitative results of our 3D object segmentation on the ScanNet dataset. OpenGaussian and InstanceGaussian rely on matching CLIP features extracted from 2D images. This approach is susceptible to feature inconsistencies arising from different mask viewpoints, often leading to incorrect matches (e.g., for the bed and chair). In contrast, our method achieves accurate 3D segmentation with sharp and well-defined boundaries.

method does not operate at the pixel level, its performance on average surpasses that of SOTA pixel-based approaches. As shown in Tab. 1, our zero-shot framework eliminates per-scene optimization and training, reducing feature storage by nearly 1000x and significantly lowering VRAM overhead. These results demonstrate that our approach delivers SOTA performance without the substantial computational overhead of previous methods. **2) Qualitative Evaluation.** Qualitative results are shown in Fig. 4. Relying on spatial clustering, OpenGaussian often yields incorrect matches with imprecise boundaries and includes irrelevant points (e.g., spatula, apple). Dr.Splat struggles with fine-grained instructions (e.g., bear nose, noodles), as its compressed CLIP features fail to capture full semantic richness, leading to interpretation errors. In contrast, our method uses uncompressed CLIP representations for linguistic precision, while our independent assignment and neutral-point handling mechanisms ensure sharp boundaries and superior performance.

4.2 OPEN-VOCABULARY 3D SEMANTIC SEGMENTATION

Settings 1) Task. The objective is to automatically extract 3D Gaussian points corresponding to input class names (e.g., wall, chair, table). The segmented Gaussian points are then converted into a point cloud to be evaluated against the ground-truth annotated point cloud. To ensure a precise correspondence between the converted point cloud and the ground truth, we disable the 3D Gaussian densification process during training. **2) Baselines.** Consistent with the object selection task, we compare our method against several recently proposed approaches: Dr.Splat (Jun-Seong et al., 2025), InstanceGaussian (Li et al., 2025), OpenGaussian (Wu et al., 2024), LangSplat-m, and LEGaussians-m. LangSplat-m and LEGaussians-m are adaptations of existing pixel-based methods (Shi et al., 2024; Qin et al., 2024), specifically modified to perform direct 3D referring op-

erations. As this task requires a direct understanding of 3D points, pixel-based methods are not applicable and are therefore excluded from our comparison. **3) Dataset.** We employ the ScanNet (Dai et al., 2017) dataset, a large-scale benchmark comprising indoor scene data with calibrated RGB-D images and 3D point clouds annotated with ground-truth semantic labels. For a fair and direct comparison, we adopt the same scenes and evaluation categories used in OpenGaussian.

Results 1) Quantitative Analysis. Tab.3 shows the performance on the ScanNet dataset using text queries for 19, 15, and 10 of its classes. The results show that our method consistently achieves SOTA segmentation performance across all scenes relative to the baselines. Notably, our method is training-free, which highlights its efficiency and precision. **2) Qualitative Analysis.** Qualitative results are presented in Fig.5. In complex scenes from ScanNet, both OpenGaussian and InstanceGaussian frequently exhibit incorrect matches, which limits their accuracy. This limitation arises from their reliance on matching masked CLIP image features, as semantic inconsistencies across different viewing angles make it difficult for such methods to achieve high-precision results. In contrast, by leveraging a VLM to acquire instance-level features, our method demonstrates correct segmentation with sharp and clear boundaries.

4.3 ABLATION STUDY

Neutral Point Processing. We ablate our neutral point processing on the LERF dataset with results in Tab. 4. Case #1 is the baseline without any filtering. Case #2 adds our entropy-based filtering. Case #3 introduces our full model, which further incorporates an opacity filter. As shown, entropy filtering alone provides a minor gain by suppressing noise, but its aggressive nature can inadvertently remove valid foreground points. Adding the opacity filter resolves this issue, achieving the highest mIoU. This demonstrates that both stages are complementary and essential for the final performance.

Instance Feature Extraction. To demonstrate the advantages of using a VLM for language feature extraction, we compare our approach with three baselines derived from the CLIP image encoder. Case #1 uses the feature from the single view with the largest mask area. Case #2 averages features from all valid views. Case #3 first renders the class foreground points onto each view and computes the IoU between the rendered foreground masks and candidate masks. We then discard the low-IoU masks and average the features of the remaining ones. The results are presented in Tab. 5. Single-view methods struggle to capture comprehensive semantics, while multi-view averaging methods often yield ambiguous features due to occlusions. Although filtering-based methods significantly improve matching accuracy, they require a rendering pass for each view, which incurs high runtime costs. Moreover, these methods can obscure discriminative details due to feature discrepancies across different views. In contrast, our VLM-based method distills these multi-view cues into a consistent textual representation, effectively capturing the nuanced attributes required for complex and abstract queries.

5 CONCLUSION AND LIMITATION

In this work, we introduced MUSplat, a training-free and plug-and-play model for open-vocabulary understanding of 3D Gaussian scenes. Our approach shifts the focus from feature learning to direct matching, supported by a back-projection mechanism for initial grouping, a neutral point process for boundary refinement, and a VLM that distills visual appearance into a robust textual representation. Evaluations on the LERF dataset and other benchmarks confirm that MUSplat delivers SOTA-level performance on point-level open-vocabulary tasks at a fraction of the computational cost. These results suggest that matching-based solutions can serve as viable alternatives to current training-based paradigms for point-level open-vocabulary understanding in 3DGS.

Table 4: Ablation on neutral point processing.

Case	Entropy Fil.	Opacity Fil.	mIoU \uparrow
#1			53.0
#2	✓		53.2
#3	✓	✓	54.3

Table 5: Ablation on feature extraction.

Case	Method	mIoU \uparrow
#1	Single-View Image Mat.	36.9
#2	Averaged Image Mat.	39.2
#3	Filtered Image Mat.	50.1
#4	VLM-Text Mat. (Ours)	54.3

Despite its strong performance, our method has certain limitations: 1) The accuracy of our object-level grouping can be compromised in instances of substantial inaccuracies in the initial segmentation masks from SAM. 2) On rare occasions, the VLM may assign incorrect semantic labels to objects within the masks. Addressing these edge cases offers promising avenues for future research.

REFERENCES

- Jiazhong Cen, Xudong Zhou, Jiemin Fang, Changsong Wen, Lingxi Xie, Xiaopeng Zhang, Wei Shen, and Qi Tian. Tackling view-dependent semantics in 3D language gaussian splatting. arXiv preprint arXiv:2505.24746, 2025.
- Zhe Chen, Jiannan Wu, Wenhai Wang, Weijie Su, Guo Chen, Sen Xing, Muyan Zhong, Qinglong Zhang, Xizhou Zhu, Lewei Lu, Bin Li, Ping Luo, Tong Lu, Yu Qiao, and Jifeng Dai. Internvl: Scaling up vision foundation models and aligning for generic visual-linguistic tasks. arXiv preprint arXiv:2312.14238, 2024.
- Gheorghe Comanici et al. Gemini 2.5: Pushing the Frontier with Advanced Reasoning, Multimodality, Long Context, and Next Generation Agentic Capabilities. arXiv preprint arXiv:2507.06261, 2025.
- Angela Dai, Angel X Chang, Manolis Savva, Maciej Halber, Thomas Funkhouser, and Matthias Nießner. Scannet: Richly-annotated 3d reconstructions of indoor scenes. In *Proceedings of the IEEE conference on computer vision and pattern recognition*, pp. 5828–5839, 2017.
- Hao-Shu Fang, Minghao Gou, Chenxi Wang, and Cewu Lu. Robust grasping across diverse sensor qualities: The graspnet-1billion dataset. *The International Journal of Robotics Research*, 2023.
- Kim Jun-Seong, GeonU Kim, Kim Yu-Ji, Yu-Chiang Frank Wang, Jaesung Choe, and Tae-Hyun Oh. Dr. splat: Directly referring 3D gaussian splatting via direct language embedding registration. In *Proceedings of the Computer Vision and Pattern Recognition Conference*, pp. 14137–14146, 2025.
- Bernhard Kerbl, Georgios Kopanas, Thomas Leimkühler, and George Drettakis. 3D Gaussian Splatting for Real-Time Radiance Field Rendering. arXiv preprint arXiv:2308.04079, 2023. arXiv:2308.04079.
- Justin* Kerr, Chung Min* Kim, Ken Goldberg, Angjoo Kanazawa, and Matthew Tancik. Lerf: Language embedded radiance fields. In *International Conference on Computer Vision (ICCV)*, 2023.
- Alexander Kirillov, Eric Mintun, Nikhila Ravi, Hanzi Mao, Chloe Rolland, Laura Gustafson, Tete Xiao, Spencer Whitehead, Alexander C. Berg, and Wan-Yen Lo. Segment anything. In *Proceedings of the IEEE/CVF international conference on computer vision*, pp. 4015–4026, 2023.
- Haijie Li, Yanmin Wu, Jiarui Meng, Qiankun Gao, Zhiyao Zhang, Ronggang Wang, and Jian Zhang. Instancegaussian: Appearance-semantic joint gaussian representation for 3D instance-level perception. In *Proceedings of the Computer Vision and Pattern Recognition Conference*, pp. 14078–14088, 2025.
- Zehao Li, Wenwei Han, Yujun Cai, Hao Jiang, Baolong Bi, Shuqin Gao, Honglong Zhao, and Zhaoqi Wang. GradiSeg: Gradient-guided gaussian segmentation with enhanced 3D boundary precision. arXiv preprint arXiv:2412.00392, 2024.
- Tao Lu, Mulin Yu, Linning Xu, Yuanbo Xiangli, Limin Wang, Dahua Lin, and Bo Dai. Scaffold-gs: Structured 3D gaussians for view-adaptive rendering. In *Proceedings of the IEEE/CVF Conference on Computer Vision and Pattern Recognition*, pp. 20654–20664, 2024.
- Yiren Lu, Yunlai Zhou, Yiran Qiao, Chaoda Song, Tuo Liang, Jing Ma, and Yu Yin. Segment then splat: A unified approach for 3D open-vocabulary segmentation based on gaussian splatting. arXiv preprint arXiv:2503.22204, 2025.

- Jacob Munkberg, Jon Hasselgren, Tianchang Shen, Jun Gao, Wenzheng Chen, Alex Evans, Thomas Müller, and Sanja Fidler. Extracting triangular 3d models, materials, and lighting from images. In *Proceedings of the IEEE/CVF Conference on Computer Vision and Pattern Recognition*, pp. 8280–8290, 2022.
- Minghan Qin, Wanhua Li, Jiawei Zhou, Haoqian Wang, and Hanspeter Pfister. Langsplat: 3D language gaussian splatting. In *Proceedings of the IEEE/CVF Conference on Computer Vision and Pattern Recognition*, pp. 20051–20060, 2024.
- Yansong Qu, Shaohui Dai, Xinyang Li, Jianghang Lin, Liujuan Cao, Shengchuan Zhang, and Rongrong Ji. GOI: Find 3D gaussians of interest with an optimizable open-vocabulary semantic-space hyperplane. In *Proceedings of the 32nd ACM International Conference on Multimedia*, Melbourne VIC Australia, 2024. ACM. ISBN 979-8-4007-0686-8. doi: 10.1145/3664647.3680852.
- Alec Radford, Jong Wook Kim, Chris Hallacy, Aditya Ramesh, Gabriel Goh, Sandhini Agarwal, Girish Sastry, Amanda Askell, Pamela Mishkin, and Jack Clark. Learning transferable visual models from natural language supervision. In *International conference on machine learning*, pp. 8748–8763. PmLR, 2021.
- QiuHong Shen, Xingyi Yang, and Xinchao Wang. Flashsplat: 2d to 3d gaussian splatting segmentation solved optimally. In *European Conference on Computer Vision*, pp. 456–472. Springer, 2024.
- Jin-Chuan Shi, Miao Wang, Hao-Bin Duan, and Shao-Hua Guan. Language embedded 3D gaussians for open-vocabulary scene understanding. In *Proceedings of the IEEE/CVF Conference on Computer Vision and Pattern Recognition*, pp. 5333–5343, 2024.
- Jovana Videnovic, Alan Lukezic, and Matej Kristan. A distractor-aware memory for visual object tracking with sam2. In *Proceedings of the Computer Vision and Pattern Recognition Conference*, pp. 24255–24264, 2025.
- Yanmin Wu, Jiarui Meng, Haijie Li, Chenming Wu, Yahao Shi, Xinhua Cheng, Chen Zhao, Haocheng Feng, Errui Ding, Jingdong Wang, et al. Opegaussian: Towards point-level 3d gaussian-based open vocabulary understanding. *Advances in Neural Information Processing Systems*, 37:19114–19138, 2024.
- Mingqiao Ye, Martin Danelljan, Fisher Yu, and Lei Ke. Gaussian grouping: Segment and edit anything in 3D scenes. In *European conference on computer vision*, pp. 162–179. Springer, 2024.
- Jiaxin Zhang, Junjun Jiang, Youyu Chen, Kui Jiang, and Xianming Liu. Cob-gs: Clear object boundaries in 3dgs segmentation based on boundary-adaptive gaussian splitting. In *Proceedings of the Computer Vision and Pattern Recognition Conference*, 2025.
- Shijie Zhou, Haoran Chang, Sicheng Jiang, Zhiwen Fan, Zehao Zhu, DeJia Xu, Pradyumna Chari, Suya You, Zhangyang Wang, and Achuta Kadambi. Feature 3Dgs: Supercharging 3d gaussian splatting to enable distilled feature fields. In *Proceedings of the IEEE/CVF Conference on Computer Vision and Pattern Recognition*, pp. 21676–21685, 2024.